Josephson tunnelling of a phase-imprinted Bose–Einstein condensate in a time-dependent double-well potential

2004 New J. Phys. 6 42

(http://iopscience.iop.org/1367-2630/6/1/042)

New Journal of Physics
An Institute of Physics and Deutsche Physikalische Gesellschaft Journal

Josephson tunnelling of a phase-imprinted Bose–Einstein condensate in a time-dependent double-well potential

E Sakellari[1], **N P Proukakis, M Leadbeater and C S Adams**
Department of Physics, University of Durham, Durham DH1 3LE, UK
E-mail: Eleni.Sakellari@durham.ac.uk

New Journal of Physics **6** (2004) 42
Received 23 October 2003
Published 8 April 2004
Online at http://www.njp.org/
DOI: 10.1088/1367-2630/6/1/042

Abstract. This paper discusses the feasibility of experimental control of the flow direction of atomic Bose–Einstein condensates in a double-well potential using phase imprinting. The flow is induced by the application of a time-dependent potential gradient, providing a clear signature of macroscopic quantum tunnelling in atomic condensates. By studying both initial-state preparation and subsequent tunnelling dynamics, we find the parameters to optimize the phase-induced Josephson current. We find that the effect is largest for condensates of up to a few thousand atoms, and is only weakly dependent on trap geometry.

Contents

[1] Author to whom any correspondence should be addressed.

PII: S1367-2630(04)70914-3

1. Introduction

The creation of superconducting [1] and superfluid [2] weak links has led to the experimental observation of Josephson effects [3], arising as a result of macroscopic quantum phase coherence. Josephson weak links are typically created by connecting two initially independent superconducting or superfluid systems via a barrier with dimensions of the order of the system healing length. Such junctions lead to a variety of interesting phenomena [4], including dc- and ac-Josephson effects. Observations in superconductors preceded those in superfluids, due to the much larger healing lengths, thus enabling easier fabrication of weak links. Evidence for Josephson-like effects has been observed in ^{4}He weak links [5], and unequivocally demonstrated for weakly coupled ^{3}He systems [6]. The recent achievement of dilute trapped atomic Bose–Einstein condensation (BEC) [7] gives rise to a new system for studying Josephson effects. In particular, such systems enable the investigation of dynamical regimes not easily accessible with other superconducting or superfluid systems. Remarkable experimental progress has led to the creation of atomic BEC Josephson junction arrays, in which the harmonically trapped atoms are additionally confined by an optical lattice potential, generated by far-detuned laser beams. Phase coherence in different wells was observed by interference experiments of condensates released from the lattice [8]. In addition, Josephson effects [9] and the control of tunnelling rate have been demonstrated [10, 11]. Alternative insight into the diverse range of Josephson phenomena can be obtained by looking at a single Josephson junction arising in a double-well system. This system has already received considerable theoretical attention, with treatments based on a two-state approximation [12]–[23], zero-temperature mean field theory [24]–[32], quantum phase models [33, 34] and instanton methods [35]. Experimentally, a double-well potential may be produced by adding a blue-detuned laser beam which induces a repulsive Gaussian barrier to a harmonic trap [36]. Atomic interferometry based on such a set-up has been reported recently [37, 38]. Alternatively, a condensate can be created directly in a magnetic double-well structure [39, 40].

In this paper, we investigate the Josephson dynamics for a phase-imprinted atomic condensate in a double-well potential under the influence of a time-dependent potential gradient. We focus on the sensitivity of the Josephson flow direction to the initial-state preparation. In particular, preparation in the odd-parity energy eigenstate combined with the application of the potential gradient leads to a flow towards a region of higher potential energy providing a clear signature of Josephson tunnelling. Flow reversal in context of the Josephson effect is well known. For example, in a superconducting π junction [41], the addition of a macroscopic phase difference $\phi = \pi$ across the superconducting weak link leads to reversal of the sign of the current [42]–[44]. Also a related effect has been predicted for condensates in optical lattices as a result of the renormalization of the mass in the lattice, based on Bloch wave analysis [45].

The superfluid analogue of a superconducting π junction is a metastable π-state, recently observed in ^{3}He weak links [46]. Atomic BEC junctions behave similarly to those of ^{3}He-B. Thus, although superconducting Josephson junctions can be mapped onto a rigid pendulum, atomic condensate tunnel junctions map onto a non-rigid pendulum [14]–[16], thus exhibiting richer oscillation modes. For example, π oscillations arise in such systems [14]–[17], [34]. For an atomic condensate in a double-well potential, π-oscillation modes can be produced by imprinting a phase shift of π between the two wells. We study how these modes behave under the action of an external potential difference.

The paper is structured as follows. Section 2 introduces our main formalism, and briefly reviews the low-lying states of a condensate in a double well, whereas section 3 discusses the

dynamics associated with particular initial states, including the π-oscillation modes, under the addition of a time-dependent potential gradient. The experimental observation of controlling the Josephson flow direction by phase imprinting in current BEC set-ups is analysed in section 4, with a short conclusion in section 5.

2. Time-independent properties of a BEC in a double-well potential

At low temperatures, the behaviour of a Bose–Einstein condensate is accurately described by a non-linear Schrödinger equation known as the Gross–Pitaevskii (GP) equation. Throughout this paper, we work in dimensionless (harmonic oscillator) units, by applying the following scalings: space co-ordinates transform according to $\boldsymbol{r}_i' = a_\perp^{-1}\boldsymbol{r}_i$, time $t' = \omega_\perp t$, condensate wavefunction $\psi'(\boldsymbol{r}', t') = \sqrt{a_\perp^3}\psi(\boldsymbol{r}, t)$ and energy $E' = (\hbar\omega_\perp)^{-1}E$. Here $a_\perp = \sqrt{\hbar/m\omega_\perp}$ is the harmonic oscillator length in the transverse direction(s), where $\omega_\perp$ is the corresponding trapping frequency. We thus obtain the following dimensionless GP equation (henceforth primes are neglected for convenience) describing the evolution of the condensate wavefunction (normalized to unity)

$$\mathrm{i}\partial_t\psi(\boldsymbol{r}, t) = [-\tfrac{1}{2}\nabla^2 + V(\boldsymbol{r}) + \tilde{g}|\psi(\boldsymbol{r}, t)|^2]\psi(\boldsymbol{r}, t). \tag{1}$$

The atom–atom interaction is parametrized by $\tilde{g} = g/(a_\perp^3\hbar\omega_\perp)$, where $g = \mathcal{N}(4\pi\hbar^2 a/m)$ is the usual three-dimensional scattering amplitude, defined in terms of the s-wave scattering length a, and $\mathcal{N}$ is the total number of atoms (mass m). The total confining potential (see figure 1(a)) is given by

$$V(\boldsymbol{r}) = \tfrac{1}{2}[(x^2 + y^2) + \lambda^2 z^2] + h\exp[-(z/w)^2] + \delta z. \tag{2}$$

The first term describes a cylindrically symmetric harmonic trapping potential, with a trap aspect ratio $\lambda = \omega_z/\omega_\perp$. The trap is spherical for $\lambda = 1$, 'cigar-shaped' for $\lambda < 1$ and 'pancake-like' for $\lambda > 1$. The second term describes a Gaussian potential of height h generated by a blue detuned light sheet of beam waist w in the z direction, located at $z = 0$. In equation (2), the contribution δz corresponds to an additional linear potential of gradient δ pivoted at the centre of the trap. For $\delta > 0$, the right well obtains higher potential energy and the trap centre is additionally shifted into the $z > 0$ region; however, this shift is negligible for the parameters studied throughout this work, and will be henceforth ignored.

The eigenestates of the double-well condensate are calculated by substituting $\psi(\boldsymbol{r}, t) = \mathrm{e}^{-\mathrm{i}\mu t}\phi(\boldsymbol{r})$ and solving the resulting time-independent equation as discussed in [32]. As is well-known, sufficiently large interactions lead to the appearance of a loop structure (see e.g. [20, 47]). The loop structure for the first excited state is shown in figure 1(b). The corresponding wavefunctions for ground and first excited state are shown in figure 1(c) for $\delta = 0$. The three eigenstates are (i) a symmetric ground state Ψ_g with equal population in both wells, (ii) an anti-symmetric state with equal population in both wells and a phase difference of π across the trap centre, which we shall henceforth refer to as Ψ_e and (iii) two higher energy 'self-trapped' states with most of the population in either the left (dotted) or the right (dashed) well [13]–[15], [32]. This paper is mainly concerned with states Ψ_g and Ψ_e and superpositions thereof. In particular, we will show that the dynamics of excited states in the presence of a time-dependent potential δz are remarkably different from that of the ground state, and offer a clear demonstration of Josephson tunnelling.

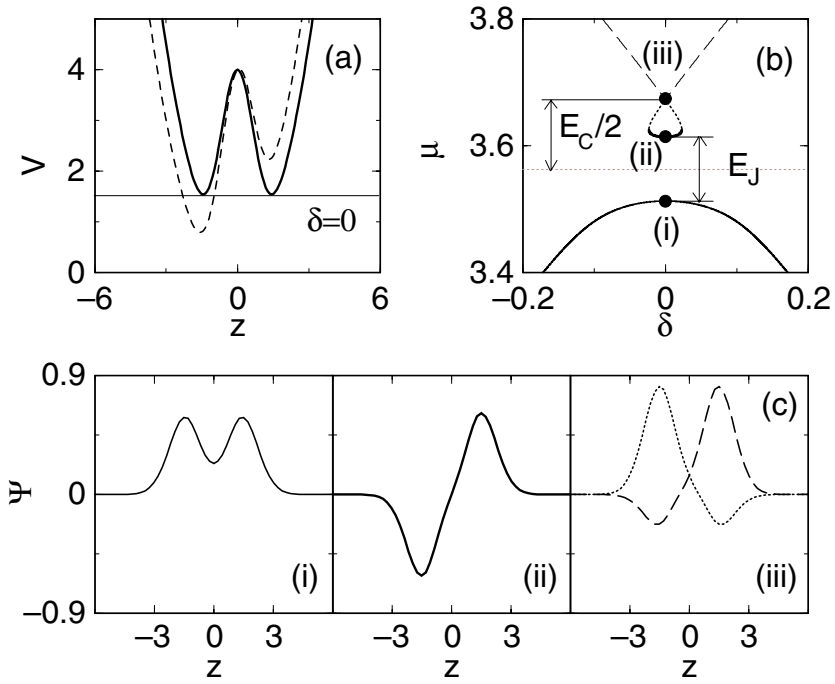

Figure 1. Double-well potential with corresponding eigenenergies and eigenstates. (a) Schematic geometry of the total confining potential in the axial direction for a Gaussian barrier (height $h = 4\hbar\omega_\perp$, waist $w = a_\perp$) located at the centre of the trap: ——, symmetric ($\delta = 0$); - - - -, asymmetric ($\delta = 0.5(\hbar\omega_\perp/a_\perp)$). (b) Eigenenergies for the double well as a function of the potential gradient δ indicating the self-interaction energy, E_C, and the Josephson coupling energy, E_J. The horizontal dotted grey line corresponds to the zero energy of the two-state model. The parameters used here are $\tilde{g} = \pi$ and spherical trap geometry ($\lambda = 1$) corresponding to $E_C = 0.220\hbar\omega_\perp$ and $E_J = 0.102\hbar\omega_\perp$. (c) Corresponding eigenstates of (b) at $\delta = 0$: (i) ground state (shown by lower —— in (b)), (ii) anti-symmetric first-excited state with equal population in both wells (——), (iii) first excited state with unequal populations, having more population in the left well (· · · · · ·) or in the right well (- - - -).

3. Tunnelling dynamics under a time-dependent magnetic field gradient

The main theme of the present study is to consider the tunnelling of states with initial phase $\phi = 0$ and π, whose symmetry is broken by the addition of a time-dependent potential gradient which increases linearly. The potential gradient is applied at $t = 0$, i.e. $\delta = Rt$ for $t > 0$ (dashed line in figure 1(a) showing the right well with higher potential energy than the left).

Before considering the effect of asymmetry, we review the behaviour of the symmetric double well. The solution of the GP equation in a double-well potential can be mapped onto a two-state model [12]–[32] by writing the wavefunction as a superposition of states localized in the left and right wells, $\psi_\ell(\boldsymbol{r})$ and $\psi_r(\boldsymbol{r})$, i.e.

$$\Psi(\boldsymbol{r}, t) = c_\ell(t)\psi_\ell(\boldsymbol{r}) + c_r(t)\psi_r(\boldsymbol{r}). \tag{3}$$

The Hamiltonian for this two-state system is

$$H = \frac{1}{2}\begin{bmatrix} -\Delta + E_C N & -E_J \\ -E_J & \Delta - E_C N \end{bmatrix}, \tag{4}$$

where $N = (N_\ell - N_r)/\mathcal{N}$ is the fractional population difference between the left and right well, Δ is the potential energy difference between the left and right wells ($\Delta = \alpha\delta$, where α is a numerical factor determined numerically from the GP solution), $E_C = \tilde{g}\langle\psi_{\ell,r}||\psi_{\ell,r}|^2|\psi_{\ell,r}\rangle$ is the self-interaction energy, $E_J = -2\langle\psi_\ell|(-\frac{1}{2}\nabla^2 + V_{\delta=0})|\psi_r\rangle$ is the Josephson coupling energy. The energy splittings E_C and E_J are indicated in figure 1(b). By writing $c_i = \sqrt{N_i}\exp(i\phi_i)$ and defining a relative phase $\phi = \phi_\ell - \phi_r$, the two-state Schrödinger equation can be rewritten in terms of the coupled equations

$$\dot{N} = E_J\sqrt{1-N^2}\sin\phi \quad \text{and} \quad \dot{\phi} = \Delta - NE_C - \frac{E_J N}{\sqrt{1-N^2}}\cos\phi. \tag{5}$$

To find the dynamics of N and ϕ, one needs to know the values of E_C, E_J and Δ for any particular barrier height, asymmetry and non-linearity. Below (figure 3) we confirm that the two-state model is an excellent approximation to the full solution of the Schrödinger equation as long as $|\delta|$ is not too large.

If a system is initially prepared in one of its eigenstates, Ψ_g or Ψ_e, it will remain in that same state and there is no tunnelling current. This is shown in figure 2(a), where we plot the fractional relative population N as a function of time with $\delta = 0$ for $t < 0$. However, if the system is prepared in a superposition of Ψ_g or Ψ_e with a π phase difference, i.e.

$$\Psi_{\pi\pm} = \frac{1}{\sqrt{2}}(\Psi_g \pm \Psi_e), \tag{6}$$

the population tunnels back and forth (see figures 2(b) and (c)) and the relative phase between the two wells oscillates around a mean value of π (π oscillations [14]–[17], [34]). The amplitude of the π oscillations depends on the ratio $\Lambda = E_C/E_J$ [15]–[17], [26, 28, 29]. By solving the two-state coupled equations (5) with initial conditions $N(0) = 0.994$ (determined from the GP solution for $\psi_{\pi-}$) and $\phi(0) = \pi$, we find a critical ratio, $\Lambda_c \sim 1.80$. For $\Lambda < \Lambda_c$, the population oscillates between $\pm N(0)$, as in figure 2(b) ($t < 0$), whereas for $\Lambda > \Lambda_c$ the oscillations in N are suppressed (figure 2(c) ($t < 0$)). Note that in figure 2(b), we have shifted the time origin by a quarter of an oscillation period such that $N = 0$ at $t = 0$.

The effect of introducing an asymmetry depends sensitively on the initial state. For Ψ_g, the potential gradient induces a Josephson current to the left (lower potential energy region), whereas for Ψ_e flow occurs to the right (higher potential energy) (figure 2(a)). The situation is more complex for superposition states, such as $\Psi_{\pi\pm}$. For $\Lambda < \Lambda_c$, if the potential gradient is turned on rapidly (compared with the period of the π oscillations), the oscillations in N are suppressed tending towards a mean N close to its initial value (figure 2(b)). For $\Lambda > \Lambda_c$, the induced flow is very different for $\Psi_{\pi+}$ and $\Psi_{\pi-}$. For $\Psi_{\pi+}$ most of the population remains self-trapped in the higher energy well, whereas for $\Psi_{\pi-}$ a large fraction of the population flows from the lower to the upper well.

The parameters used throughout the rest of the paper, $\tilde{g} = \pi$ and a spherical trap geometry ($\lambda = 1$), give $E_C = 0.220\hbar\omega_\perp$ and $E_J = 0.102\hbar\omega_\perp$, corresponding to the regime, $\Lambda > \Lambda_c$. In this

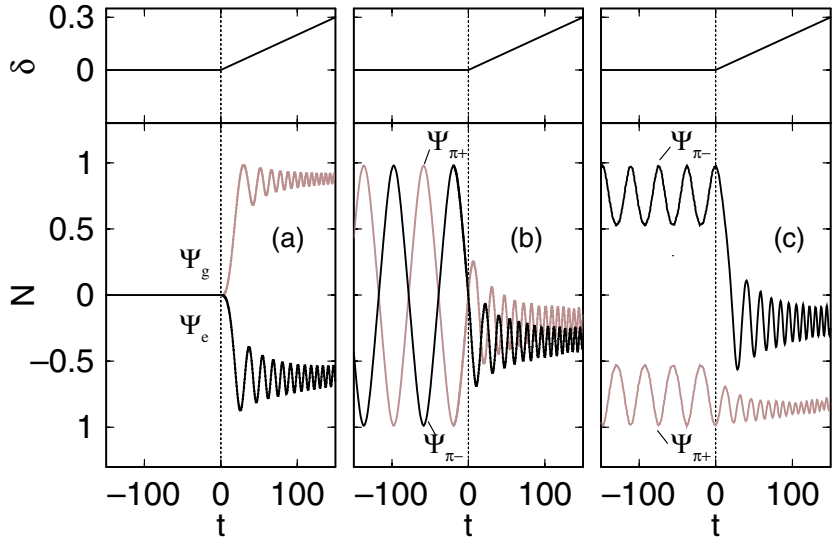

Figure 2. Evolution of fractional population difference N as a function of time (calculated using the GP equation) without ($t < 0$) and with ($t > 0$) a potential gradient $\delta = Rt$ (shown at the top of each figure) for different initial states: (a) a pure ground Ψ_g or first excited Ψ_e state with equal populations in both wells. In this case, tunnelling only arises due to the additional external potential; (b) the superposition states $\Psi_{\pi\pm}$ for $\tilde{g} = \pi/2$, corresponding to the regime $\Lambda < \Lambda_c$ ($E_C = 0.123\hbar\omega_\perp$ and $E_J = 0.095\hbar\omega_\perp$), showing maximum amplitude π oscillations for $t < 0$: and (c) the superposition states $\Psi_{\pi\pm}$ for $\tilde{g} = \pi$, corresponding to $\Lambda > \Lambda_c$ ($E_C = 0.220\hbar\omega_\perp$ and $E_J = 0.102\hbar\omega_\perp$). The other parameters used here are $\lambda = 1$, $h = 4\hbar\omega_\perp$ and $R = 2 \times 10^{-3}(\hbar\omega_\perp^2/a_\perp)$. Time is measured in units of $\omega_\perp^{-1}$.

regime, the experimental preparation of $\Psi_{\pi\pm}$ from the ground state is more difficult as it requires a transfer of population in addition to imprinting a phase difference of π. However, as we will see in section 4, straightforward phase imprinting can generate a superposition that contains a large fraction of $\Psi_{\pi\pm}$.

The tunnelling behaviour of different initial states such as Ψ_g and Ψ_e under a potential gradient can be explained in terms of the time-independent solutions [32]. These can be plotted as a function of time via their dependence on the time-dependent potential gradient $\delta = Rt$. The time evolution and the corresponding time-independent population difference for state Ψ_e is shown in figure 3(a), from which it is found that, for slow velocities, the system follows the eigenstate almost adiabatically. The initial dynamics discussed above is also well described by the two-state model [12]–[23] (grey line in figure 3(a)). However, for larger gradients, the full potential GP calculation predicts that the atoms return to the lower (or left) potential well, as illustrated by the density snapshots in figure 3(b), whereas the two-state model suggests they remain in the upper (right) well. This breakdown of the two-state model occurs because it does not take higher-lying modes into consideration [32]. This is an important consideration for any experimental demonstration of macroscopic flow to the higher well.

The flow towards the right (higher) potential well, shown in figure 3(b), provides a clear macroscopic demonstration of quantum tunnelling. To consider whether this effect is observable in current experimental set-ups, we have studied the effect of varying the non-linearity, trap

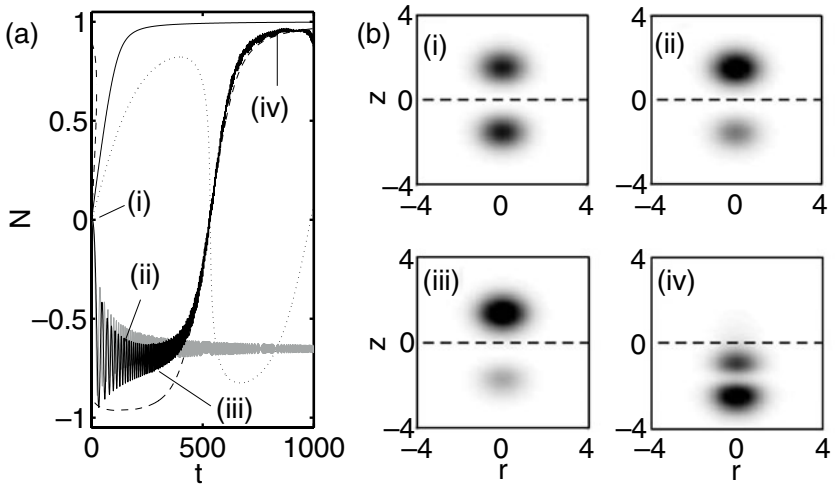

Figure 3. (a) Evolution of fractional population difference N as a function of time, for a system initially prepared in state Ψ_e based on the Gross–Pitaevskii equation (black line) and the two-state model, equation (5) (grey line) with initial condition $N(0) = 0$ and $\phi(0) = \pi$. The fractional population differences for the eigenstates are also plotted for the ground (——), first excited (- - - -) and second excited states ($\cdots\cdots$). Here $h = 4\hbar\omega_\perp$, $\lambda = 1$, $\tilde{g} = \pi$ and the potential gradient $\delta = Rt$ increases at constant rate $R = 10^{-3}(\hbar\omega_\perp^2/a_\perp)$. (b) Snapshots of the evolution of the density distribution for case (a) when (i) $t = 0$, (ii) 100, (iii) 300 and (iv) 800 in units of $(\omega_\perp^{-1})$. The population of both wells is initially equal ($t = 0$). As the gradient is increased in (ii) and (iii), population starts being transferred towards the right ($z > 0$) (upper well). Increasing the asymmetry beyond a threshold value leads the population to be once again transferred to the left ($z < 0$) (lower well)—not shown explicitly here. Eventually, (iv), a transition to the second excited state occurs (d) (see movie).

geometry and the time dependence of the ramp. Note that, the effect of interactions has also been considered in [27], with the effective interaction also modified by atom losses [22]. Our studies reveal that increasing the non-linearity causes a reduction in the amount of initial flow to the upper well, and thus tends to inhibit the experimental observation (see the next section for experimental estimates). For example, using the parameters of figure 3 with a non-linearity 10 times larger (i.e. $\tilde{g} = 10\pi$) leads to a reduction of the average population imbalance induced by the applied potential gradient of slightly more than a factor of 2. It is thus natural to ask if other factors (e.g. modifying initial trap aspect ratio or changing barrier height h) will have the opposite effect. Enhanced tunnelling has been predicted for 'pancake' traps ($\lambda > 1$) [28]. Furthermore, such geometries feature a larger energy splitting between the ground and first excited state, making them more robust to external perturbations (e.g. thermal [18, 21, 23, 48]). However, the suppression of tunnelling induced by increased non-linearities cannot be compensated by changing the geometry. We should further comment on the extent to which the above findings depend on the rate R with which the linear potential gradient $\delta = Rt$ is applied. Figure 3(a) shows the dependence for $R = 10^{-3}(\hbar\omega_\perp^2/a_\perp)$. If R is increased by a factor of 10, then the maximum flow to the right well is reduced by roughly a factor of 2. Also flow to higher potential region can only be observed for approximately one-tenth of the time, unless the gradient is ramped up

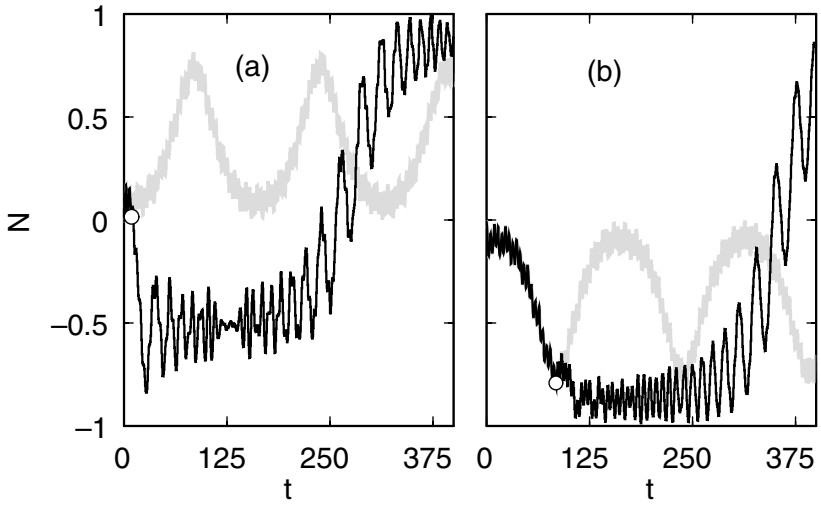

Figure 4. Evolution of fractional population difference N as a function of time for initial states prepared by phase imprinting ($|\alpha| = \hbar\omega_\perp$, $\tau_0 = 3\omega_\perp^{-1}$). The grey and black curves correspond respectively to the absence of a potential gradient (i.e. symmetric double well), and the addition of a potential gradient $\delta = R(t - \tau_1)$ increased linearly at rate $R = 2 \times 10^{-3}(\hbar\omega_\perp^2/a_\perp)$ from time τ_1, with this time indicated by the open circles: (a) $\alpha = \hbar\omega_\perp$, $\tau_1 = 10\omega_\perp^{-1}$ and (b) $\alpha = -\hbar\omega_\perp$, $\tau_1 = 85\omega_\perp^{-1}$. Other parameters as in figure 2(c).

to a particular value and subsequently kept constant. If the gradient is kept constant at the point of maximum population difference, the population remains trapped in the right upper well, i.e. macroscopic quantum self-trapping [13]–[15], [49] occurs to a state with higher potential energy. In this regime, where the gradient does not exceed the value at which the flow is reversed, the two-state model correctly predicts the behaviour.

4. Experimental considerations

We now discuss the feasibility of observing flow to the upper well using phase imprinting [50, 51]. Starting from the condensate ground state in a symmetric double-well trap, population can be transferred to the excited states by applying a light-induced potential of the form

$$V_r(z, t) = \alpha \sin(\pi t/\tau_0) \tanh(z) \qquad \text{for } t < \tau_0, \tag{7}$$

where α and τ_0 are constants which we vary. At $t = \tau_0$, the potential V_r is suddenly switched off such that there is a π phase shift between the two wells. This simple phase-imprinting method does not distinguish between states with similar density and phase profiles such as Ψ_e or $\Psi_{\pi\pm}$. Other more sophisticated methods of preparing the initial state such as two-photon adiabatic passage [52] could also be explored.

We choose the phase-imprinting parameters such that the amplitudes of the subsequent number oscillations between the wells in a symmetric double-well potential (i.e. in the absence of a potential gradient) are minimized. The time dynamics for this case are shown by the grey lines in figure 4, and essentially correspond to π oscillations with $\langle N(t)\rangle \neq 0$, as discussed in

[14]–[17], [34] and shown in figure 2(c). For an imprinted phase of π, the population oscillates with most of the condensate in the left well (grey line in figure 4(a)), whereas for an imprinted phase of $-\pi$, the population oscillations are contained within the right well (grey line in figure 4(b)). In both cases, the addition of the potential gradient at a time τ_1 indicated by the open circles in figure 4, induces a flow to the right or upper potential well (solid lines in figure 4). Even at the time in the π-oscillation cycle when most of the population is already on the right well and would subsequently flow back to the left, the addition of the gradient induces more flow to the right, as shown in figure 4(b). Note that, in this case, the population remains trapped in the right well until the influence of the second excited state becomes important. If the correct initial-state parameters are obtained from the full GP calculation, then the results shown in figure 4 can be reproduced using the two-state model, except for the transition to the second excited state. However, a full potential calculation is required to correctly predict the initial state and the dynamics for larger potential gradients, when the two-state model breaks down.

Finally, we discuss typical experimental parameters required for the demonstration of Josephson flow to the upper potential well. The number of atoms is given by

$$\mathcal{N} = \frac{\tilde{g}}{4\pi}\frac{a_\perp}{a} = \frac{\tilde{g}}{4\pi a}\sqrt{\frac{\hbar}{m\omega_\perp}}. \tag{8}$$

The total atom number is independent of the trap aspect ratio; therefore, for given dimensionless non-linearity $\tilde{g}$, large atom numbers can be obtained for light, weakly interacting, transversally weakly confined systems. For a large number of atoms, one should preferably choose species with a small value of $a\sqrt{m}$. For example, taking $\tilde{g} = 4\pi$ and $\omega_\perp = 2\pi \times 5\,\mathrm{Hz}$, we find $\mathcal{N} = 3300$ (^{23}Na) and 1000 (^{87}Rb). An enhancement of the atom number by a factor of 10 may be possible by tuning around a Feshbach resonance (e.g. ^{23}Na, ^{85}Rb and ^{133}Cs) [53]. For ^{7}Li and ^{85}Rb, the number of atoms needed to observe such Josephson flow will not probably exceed the critical value [54] for collapse.

Note that for fixed, reasonably small, non-linearity ($\tilde{g} < 10\pi$), such that the effect can be clearly observed, one needs weak transverse confinement $\omega_\perp$ to obtain a reasonable number of atoms which can be imaged easily. However, small $\omega_\perp$ imply long timescales, such that the observation of this effect becomes limited by other factors (e.g. thermal damping [18, 21, 23, 48], atom losses [22] etc). If we choose $\omega_\perp = 2\pi(5\text{–}100)$ Hz, then the preparation of the Ψ_e state requires a time $\tau_0 \sim 300\text{–}150$ ms and an applied field gradient $R = (10^{-3}\text{–}10^{-2})(\hbar\omega_\perp/a_\perp)$ (which translates into a Zeeman shift of 1–100 MHz cm^{-1} ramped up over a total experimental time $t_{\mathrm{exp}} \sim 1.5\,\mathrm{s}\text{–}75\,\mathrm{ms}$).

5. Conclusions

We have studied the Josephson dynamics of phase-imprinted condensates in a double-well potential in the presence of a time-dependent potential gradient. We show that phase imprinting can lead to a significant change in the flow direction producing a clear signature of macroscopic quantum tunnelling. We have discussed the range of parameters for optimum experimental demonstration of this effect, and find that it is only weakly dependent on the aspect ratio of the trap. However, suppression of the flow for large non-linearities restricts the condensate size to a few thousand atoms. An attractive candidate for the observation of the flow reversal is the recently

realized atom chips [55] with a blue detuned laser beam to create the weak link. The observation of the flow of phase-imprinted states would provide a clear experimental demonstration of the Josephson effect.

Acknowledgments

We acknowledge funding from the UK EPSRC.

References

[1] Likharev K K 1979 *Rev. Mod. Phys.* **51** 101
[2] Davis J C and Packard R E 2002 *Rev. Mod. Phys.* **74** 741
[3] Josephson B D 1962 *Phys. Rev. Lett.* **1** 251
[4] Barone A and Paterno G 1982 *Physics and Applications of the Josephson Effect* (New York: Wiley)
[5] Sukhatme K, Mukharsky Yu, Chul T and Pearson D 2001 *Nature* **411** 280
[6] Avenel O and Varoquaux E 1988 *Phys. Rev. Lett.* **60** 416
Pereverzev S V, Loshak A, Backhaus S, Davis J C and Packard R E 1997 *Nature* **388** 449
Backhaus S, Pereverzev S V, Loshak A, Davis J C and Packard R E 1997 *Science* **278** 1435
[7] Anderson M H *et al* 1995 *Science* **269** 198
Davis K B *et al* 1995 *Phys. Rev. Lett.* **75** 3969
Bradley C C *et al* 1997 *Phys. Rev. Lett.* **75** 1687
Bradley C C *et al* 1997 *Phys. Rev. Lett.* **79** 1170
Fried D G *et al* 1998 *Phys. Rev. Lett.* **81** 3811
Robert A *et al* 2001 *Science* **292** 461
Dos Santos F P *et al* 2001 *Phys. Rev. Lett.* **86** 3459
Yosuke T, Maki K, Komori K, Takano T, Honda K, Kumakura M, Yabuzaki T and Takahashi Y 2003 *Phys. Rev. Lett.* **91** 040404
[8] Anderson B P and Kasevich M A 1998 *Science* **282** 1686
Orzel C, Tuchman A K, Fenselau M L, Yasuda M and Kasevich M A 2001 *Science* **291** 2386
[9] Cataliotti F S, Burger S, Fort C, Maddaloni P, Minardi F, Trombettoni A, Smerzi A and Inguscio M 2001 *Science* **293** 843
[10] Denschlag J H, Simsarian J E, Häffner H, McKenzie C, Browaeys A, Cho D, Helmerson K, Rolston S L and Phillips W D 2002 *J. Phys. B: At. Mol. Opt. Phys.* **35** 3095
[11] Greiner M, Mandel O, Esslinger T, Hänsch T W and Bloch I 2002 *Nature* **415** 39
[12] Jack M W, Collett M J and Walls D F 1996 *Phys. Rev.* A **54** R4625
[13] Milburn G J, Corney J, Wright E M and Walls D F 1997 *Phys. Rev.* A **55** 4318
[14] Smerzi A, Fantoni S, Giovanazzi S and Shenoy S R 1997 *Phys. Rev. Lett.* **79** 4950
[15] Raghavan S, Smerzi A, Fantoni S and Shenoy S R 1999 *Phys. Rev.* A **59** 620
[16] Marino I, Raghavan S, Fantoni S, Shenoy S R and Smerzi A 1999 *Phys. Rev.* A **60** 487
[17] Raghavan S, Smerzi A and Kenkre V M 1999 *Phys. Rev.* A **60** R1787
[18] Zapata I, Sols F and Leggett A 1998 *Phys. Rev.* A **57** R28
[19] Javaneinen J and Ivanov M Yu 1999 *Phys. Rev.* A **60** 2351
[20] Wu B and Niu Q 2000 *Phys. Rev.* A **61** 023402
[21] Ruostekoski J and Walls D F 1998 *Phys. Rev.* A **58** R50
[22] Kohler S and Sols F 2002 *Phys. Rev. Lett.* **89** 60403
[23] Kohler S and Sols F 2003 *New J. Phys.* **5** 94
[24] Williams J, Walser R, Cooper J, Cornell E and Holland M 1999 *Phys. Rev.* A **59** R31
[25] Salasnich L, Parola A and Reatto L 1999 *Phys. Rev.* A **60** 4171

[26] Leggett A J 1999 *Proc. 16th Int. Conf. on Atomic Physics, Windsor, Ontario, August 1998* ed W E Baylis and G F Drake (AIP Conf. Proc. No. 477) (Woodbury, NY: AIP) p 154
[27] Zobay O and Garraway B M 2000 *Phys. Rev.* A **61** 33603
[28] Williams J 2001 *Phys. Rev.* A **64** 013610
[29] Leggett A J 2001 *Rev. Mod. Phys.* **73** 307
[30] Giovanazzi S, Smerzi A and Fantoni S 2000 *Phys. Rev. Lett.* **84** 4521
[31] Menotti C, Anglin J R, Cirac J I and Zoller P 2001 *Phys. Rev.* A **63** 023601
[32] Sakellari E, Leadbeater M, Kylstra N J and Adams C S 2002 *Phys. Rev.* A **66** 033612
[33] Leggett A J and Sols F 1991 *Found. Phys.* **21** 353
[34] Anglin J R, Drummond P and Smerzi A 2001 *Phys. Rev.* A **64** 063605
[35] Zhou Y, Zhai H, Lu R, Xu Z and Chang L 2003 *Phys. Rev.* A **67** 043606
Li W-D, Zhang Yu and Liang J-Q 2003 *Phys. Rev.* A **67** 065601
[36] Andrews M R, Townsend C G, Miesner H J, Durfee D S, Kurn D M and Ketterle W 1997 *Science* **275** 637
[37] Leanhardt A E, Pasquini T, Saba M, Schirotzek A, Shin Y, Kielpinski D, Pritchard D E and Ketterle W 2003 *Science* **301** 1513
[38] Shin Y, Saba M, Pasquini T A, Ketterle W, Pritchard D E and Leanhardt A E 2004 *Phys. Rev. Lett.* **92** 050405
[39] Thomas N R, Wilson A C and Foot C J 2002 *Phys. Rev.* A **65** 063406
[40] Tiecke T G, Kemmann M, Buggle Ch, Shvarchuck I, von Klitzing W and Walraven J T M 2003 *J. Opt. B: Quantum Semiclass. Opt.* **5** S119
[41] Bulaevskii L N, Kuzii V V and Sobyanin A A 1977 *JETP Lett.* **25** 290
Geshkenbeim V B, Larkin A I and Barone A 1987 *Phys. Rev.* B **36** 235
[42] Baselmans J J A, Morpurgo A F, van Wees B J and Klapwijk T M 1999 *Nature* **397** 43
[43] Baselmans J J A, van Wees B J and Klapwijk T M 2001 *Appl. Phys. Lett.* **79** 2940
[44] Smilde H J H, Ariand, Blank D H A, Gerritsma G J, Hilgenkamp H and Rogalla H 2002 *Phys. Rev. Lett.* **88** 057004
[45] Pu H, Baksmaty L O, Zhang W, Bigelow N P and Meystre P 2003 *Phys. Rev.* A **67** 043605
[46] Backhaus S, Pereverzev S, Simmonds R W, Loshak A, Davis J C and Packard R E 1998 *Nature* **392** 687
[47] Wu B, Diener R B and Niu Q 2002 *Phys. Rev.* A **65** 025601
Diakonov D, Jensen L M, Pethick C J and Smith H 2002 *Phys. Rev.* A **66** 013604
Mueller E J 2002 *Phys. Rev.* A **66** 063603
[48] Sols F 1999 *Bose–Einstein Condensation in Atomic Gases, Proc. Int. School of Physics 'Enrico Fermi', Course CXL, Varenna on Lake Como, July 1998* ed M Inguscio, S Stringari and C E Wieman (Washington, DC: Ohmsha/IOS Press) p 453
[49] Ostrovskaya E A *et al* 2000 *Phys. Rev.* A **61** 013601(R)
[50] Burger S *et al* 1999 *Phys. Rev. Lett.* **83** 5198
Denschlag J *et al* 2000 *Science* **287** 97
[51] Mahmud K W, Perry H and Reinhardt W P 2003 *J. Phys.* B **36** L265
[52] Williams J E and Holland M J 1999 *Nature* **401** 568
[53] Inouye S, Andrews M R, Stenger J, Miesner H-J, Stamper-Kurn D M and Ketterle W 1998 *Nature* **392** 151
Roberts J L, Claussen N R, Cornish S L and Wieman C E 2000 *Phys. Rev. Lett.* **85** 728
Robert A *et al* 2001 *Science* **292** 461
[54] Bradley C C, Sackett C A and Hulet R G 1997 *Phys. Rev. Lett.* **78** 985
[55] Ott H, Fortagh J, Schlotterbeck G, Grossmann A and Zimmermann C 2001 *Phys. Rev. Lett.* **87** 230401
Hänsel W, Hommelhoff P, Hänsch T W and Reichel J 2001 *Nature* **413** 498
Schneider S, Kasper A, vom Hagen Ch, Bartenstein M, Engeser B, Schumm T, Bar-Joseph I, Folman R, Feenstra L and Schiedmayer J 2003 *Phys. Rev.* A **67** 023612
Jones M P A *et al* 2003 *Phys. Rev. Lett.* **91** 080401